CHAPTER 13

POLLUTANTS IN THE SEAS AROUND US[1]

Shawn Booth,[a] **William W. L. Cheung**,[b] **Andrea P. Coombs-Wallace**,[a,c] **Vicky W. Y. Lam**,[a] **Dirk Zeller**,[a] **Villy Christensen**,[d] and **Daniel Pauly**[a]

[a]*Sea Around Us*, University of British Columbia, Vancouver, BC, Canada
[b]Changing Oceans Research Unit and NF-UBC Nereus Program, University of British Columbia, Vancouver, BC, Canada
[c]Frankfurt Zoological Society, Mpika, Zambia, and Imperial College, London
[d]Fisheries Centre, University of British Columbia, Vancouver, BC, Canada

The *Sea Around Us* was named after Rachel Carson's book of the same title (Carson 1951), and thus it is fitting that it should have undertaken various studies on the effects pollutants have on marine ecosystems, in part inspired by Carson's *Silent Spring* (Carson 1962). In this chapter, after a brief review of current issues in marine pollution, two vignettes are presented that examine pollutant dynamics in aquatic ecosystems: polychlorinated biphenyls (PCBs) in the northeast Pacific and methylmercury in the Faeroe Islands. Then, two global models are presented, one on the

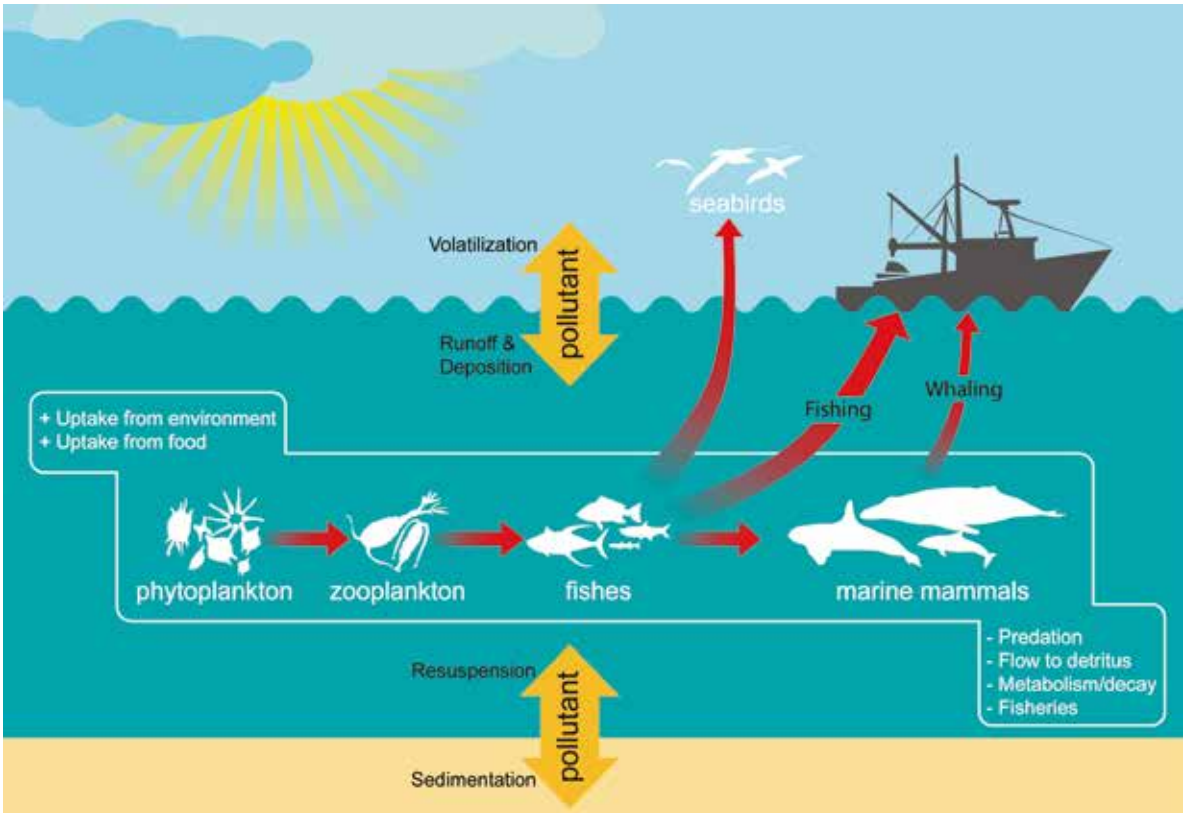

Figure 13.1. Schematic representation of how pollutants move within aquatic ecosystems; note that grazing and predation lead to bioaccumulation (see text). (Original figure by Ms. Evelyn Liu.)

BOX 13.1. THE ECOTRACER ROUTINE FOR TRACKING NUTRIENTS AND POLLUTANTS

Shawn Booth and Daniel Pauly, *Sea Around Us*, University of British Columbia, Vancouver, Canada

Ecotracer is a subroutine within the EwE modeling framework that allows the user to simulate the flow of pollutants (or nutrients such as nitrogen; see Kline and Pauly 1998) in an ecosystem by tracking the gains and losses in the functional groups and the environment. Ecotracer estimates pollutant concentrations in all functional groups, including those that may have no reported data available, and forcing functions can be used to simulate changes of pollutant inflow rates through time.

Four parameters describe the gains and losses to the environment: the initial concentration (g/km^2); the base inflow rate (g/km^2/year); the decay rate (per year), accounting for the pollutant being transformed to other substances; and the base volume exchange loss (per year). The initial environmental concentration is a snapshot affected by the base inflow rate, which can include atmospheric loading, runoff, volatilization, sedimentation, and resuspension.

Five parameters are used to describe the gains and losses in the biological groups: initial pollutant concentration per biomass (e.g., g/t), if known; direct absorption rates (e.g., grams of pollutant/tonne of biomass/environment concentration/year); decay rate (per year); assimilation as a proportion (0–1) of the exposure; and concentration of pollutant in immigrating biomass (e.g., g/t). One group must have a direct absorption rate in order for the pollutant to spread to other functional groups as determined from trophic interactions. If long-term equilibrium concentrations are sought, the initial pollutant concentration per biomass does not need to be known.

Pollutant concentrations in functional groups result from five processes: the predator–prey interactions as detailed in the EwE diet matrix; direct uptake from the environment for some organisms or diffusion across membranes; internal metabolism and decay processes, which transform the pollutant into other substances; migration effects; and fisheries, which can change the age structure of the population, resulting in changes in pollutant concentrations. Technical details are available in Christensen and Walters (2004).

REFERENCES

Christensen, V., and C. J. Walters. 2004. Ecopath with Ecosim: methods, capabilities and limitations. *Ecological Modelling* 172: 109–139.

Kline, T. C., and D. Pauly. 1998. Cross-validation of trophic level estimates from a mass-balance model of Prince William Sound using 15N/14N data. Pp. 693–702 in T. J. Quinn II, F. Funk, J. Heifetz, J. N. Ianelli, J. E. Powers, J. F. Schweigert, P. J. Sullivan, and C.-I. Zhang (eds.), *Proceedings of the International Symposium on Fishery Stock Assessment Models*. Alaska Sea Grant College Program Report No. 98-01.

bioaccumulation and concentration of dioxin in marine organisms as a result of atmospheric deposition, the other on the production, atmospheric transport, and deposition of dioxin on a global basis. Although pollution in marine waters has direct effects less often than in freshwaters, it often exacerbates the effects of other stressors, such as overfishing. Thus, the concepts, methods, and software presented herein may be useful to future students of marine pollution, especially in light of current concerns about the traceability and wholesomeness of seafood.

For a very long time it seemed true, especially for marine systems, that "the solution to pollution is dilution." However, biomagnification up the food web and bioaccumulation in long-lived organisms can effectively reverse the effect of dilution (figure 13.1), as can the sheer magnitude of the pollutant input. Thus, even the open oceans have now reached a stage where pollutants originating from various societal activities ranging from mining, manufacturing, and agriculture to consuming their products are reaching worrisome levels. Foremost is the thermal pollution and increased carbonic acid in the oceans, both the results of carbon dioxide emissions also responsible from global warming, which have profound effects on ocean life (chapter 8). Another kind of ma-

rine pollution is plastic pollution, much of it from plastic debris, some very small, which now contributes an increasing fraction of what fish (Moore 2008), marine turtles (Bugoni et al. 2001), and seabirds (chapter 10) mistakenly ingest instead of their natural prey.

The *Sea Around Us* used extensively, and further developed, ecosystem modeling tools, notably Ecopath with Ecosim (EwE; Pauly et al. 2000; Christensen and Walters 2004; chapter 9), which allow tracking of pollutants through and up a food web. This chapter thus briefly reviews the work of the *Sea Around Us* on pollutant tracking, including global models to simulate the oceanic dispersion and uptake of dioxin, whose global scale corresponds to the other issues in this volume.

Two vignettes are presented here that examine pollutant dynamics in aquatic ecosystems. The first vignette presents a model of bioaccumulation of PCBs in the eastern Bering Sea of Alaska (Coombs 2004), and the second deals with the bioaccumulation of mercury in the Faeroe Islands (Booth and Zeller 2005). The work on PCBs and mercury relied heavily on the Ecotracer routine of EwE (Christensen and Walters 2004; box 13.1).

We present two global models for dioxin, a group of chemicals that have seventeen forms with varying toxicological effects, with the most toxic form, 2,3,7,8-tetrachlorodibenzo-*p*-dioxin, being classified as a human carcinogen (IARC 1997). One examines the bioaccumulation and concentration of dioxin in marine organisms as a result of atmospheric deposition (Christensen and Booth 2006; Booth et al. 2013), and the other aims to simulate the production, atmospheric transport, and deposition of dioxin on a global basis. However, although the estimate of dioxin concentrations in marine organisms relied in part on the Ecotracer routine, the atmospheric transport model was developed outside the EwE framework.

PCBs in Alaska's Eastern Bering Sea

The eastern Bering Sea has undergone substantial ecological changes since 1950 that have affected the marine community's biomass and composition (NRC 1996). These changes have been attributed to the effects commercial whaling and fishing have had on the structure of the community (Trites et al. 1999) and to an oceanic regime shift in the late 1970s that favored the survival of one suite of species over another (Mantua et al. 1997). The area is also susceptible to depositions of pollutants that undergo long-range atmospheric transport, such as PCBs, because colder temperatures favor the entrapment of these pollutants in high-latitude areas.

PCBs are of concern because of their potential to decrease marine mammal populations in the eastern Bering Sea. Also, because many Alaskan native people consume marine mammals, they are also exposed to these toxins as part of their traditional diet. PCBs are lipophilic (fat soluble), resist degradation, persist in the environment, accumulate in marine mammal and fish tissue, are highly toxic, and can directly affect the health of animals and people. Toxic effects on marine mammals include immunosuppression, developmental abnormalities, carcinogenicity, endocrine disruption, reproductive impairment, neurotoxicity, skin disorders, tumors, and lipid degeneration (AMAP 1997; Kannan et al. 2000). Many of these effects are also observed in humans (Simmonds et al. 2002). Contaminant burdens may have greater impacts when people and animals are stressed, leading to compromised health, and in wild animals this may affect mortality levels indirectly (Loughlin and York 2000).

To gain a better understanding of the effects of these stressors, two ecosystem models were constructed using the EwE software that describe the eastern Bering Sea in the 1950s and the 1980s. Both model the accumulation of PCBs using the Ecotracer routine within EwE to assess the implications for marine mammals and people. In the Bering Sea, PCB levels rose steadily from the 1950s until the mid-1970s, when regulations restricting PCB use and production were implemented (Livingston and Low 1998), and this led to an initial

reduction of PCB concentration in wildlife, but PCB concentrations stopped declining and have stabilized since the mid-1980s (Parker and Dasher 1999). This leveling off suggests that ongoing environmental cycling and continued leakage of PCBs are sufficient to maintain concentrations at a steady state (Aguilar et al. 2002).

The models describing the composition and flows of biomass in the ecosystem were compared with biomass trends taken from systematically collected assessment data in relation to fisheries and marine mammals (Trites et al. 1999). Similarly, concentration levels of PCBs were compared with reported concentrations. For marine mammals, simulated PCB concentrations in blubber were compared with reported blubber concentrations from male animals, because approximately 90% of their PCB load accumulates in blubber (Becker 2000), and male animals accumulate PCBs throughout their life, as compared to females, which can transfer some of their burden to their fetuses and also to calves when they are nursing. For other organisms, concentrations in muscle tissue were used because of its large contribution to body mass (Aguilar et al. 1999). Only total PCBs reported as the sum of individual congeners in a sample analyzed using more accurate, sensitive, and widely recognized gas chromatography methods were included (Valoppi et al. 1998).

The onset of significant PCB input occurred in sediment layers deposited after 1950 (Iwata et al. 1993). Accordingly, PCB concentrations predicted using the 1950s model depended on bottom-up processes. For the 1950s simulation, an environmental concentration of 9.2 g/km^2 (Kawano et al. 1986) and an inflow rate of 4.7 g/km^2/year (Iwata et al. 1994) were used to initialize the model. Time series data were also included in the 1950s model to account for changes in PCB input over time as a result of increasing global PCB production before the mid-1970s. Species and functional groups were considered to lack any PCBs at initialization so that the model estimated the bioaccumulation of PCBs from a starting point of zero. Plankton and large flatfish incorporated PCBs by direct uptake from the environment, and thus these groups were considered to be the trophic entry point of PCBs. These PCBs were then transferred to the remaining biological groups via trophic interactions. Many organisms have the ability to transform PCBs in their tissues, and thus, for most groups, a decay rate was used to match the predicted PCB concentrations to observed concentrations.

For the 1980s model, environmental concentrations were increased to 65 g/km^2 (Tysban 1999) and the inflow rate was increased to 6.3 g/km^2/year (Iwata et al. 1994) to reflect the increasing impact of PCBs on the ecosystem. Plankton groups were assigned uptake rates from the environment and, as in the 1950s model, most groups were assigned a decay rate. For both models, a simulation was run over a hundred-year time period to assess the movement of PCBs within the ecosystem.

Results from the 1950s model indicated that concentrations reached their peak in the mid-1980s. Concentrations then slowly declined in a delayed response to restrictions before reaching a steady state. The 1980s model was used to forecast future PCB concentrations in the eastern Bering Sea, and similar to the 1950s model, it also predicted that concentrations reached their peak in the mid-1980s, followed by a slow decline to a steady state.

PCB concentrations in Bering Sea seawater (0.00065 µg/L) and sediment (0.13 ppb, dry weight) are two orders of magnitude lower than guidelines set by the U.S. Environmental Protection Agency (EPA) and the National Oceanic and Atmospheric Administration, respectively. The leveling off of PCB concentrations from the 1980s model suggests that ongoing environmental cycling and continued input of PCBs into the Bering Sea is sufficient to maintain concentrations at current levels. Both models suggest that, with the exception of toothed whales, concentrations in marine mammals remained between 23% (beaked whales) and 90% (walrus) lower than threshold levels throughout the time period from the 1950s to the present (table 13.1). However, the

Table 13.1. Estimated trophic level, highest concentration of PCB reached during the 1950s simulation, and the percentage difference between the range of the lower (7 ppm) and upper (15 ppm) threshold values established by Kannan et al. (2000) for the marine mammal groups modeled in the eastern Bering Sea model. Toothed whales are the only group that falls within immunosuppression threshold range.

Group	Trophic level	Concentration (ppm)	± Lower	± Upper
Sperm whales	4.75	1.9	−72.9	−87.3
Beaked whales	4.59	5.4	−22.9	−64.0
Toothed whales	4.36	11.3	+61.4	−24.7
Steller sea lions	4.30	1.9	−72.9	−87.3
Seals	4.01	1.2	−82.9	−92.0
Baleen whales	3.61	1.6	−77.1	−89.3
Walrus or bearded seals	3.52	0.6	−91.4	−96.0

functional group "toothed whales" was within the 7 to 15 mg/kg wet weight threshold level established by Kannan et al. (2000).

Animals taken for subsistence from the eastern Bering Sea ecosystem are primarily from trophic levels 3 and 4. The results suggested that the greatest flow and concentrations of PCBs also occur at these trophic levels, with predicted concentrations in marine mammals and fish ranging from 0.005 to 2.15 ppm. Given that marine mammals and fish constitute a large proportion of the traditional Aleut diet, these concentrations, being well above EPA guidelines, represent a considerable contaminant risk for subsistence consumers. Perhaps the greatest contaminant concern for Alaskan natives is that PCB concentrations in their traditional foods are no longer declining, and the full extent of long-term chronic exposure for marine mammals and humans has yet to be realized (Carson 1962; Tanabe 2002).

MERCURY IN THE FAEROE ISLANDS

The Faeroe Islands are located in the North Atlantic Ocean southeast of Iceland, and their inhabitants have always relied heavily on marine resources for their livelihood and food security. In the early 2000s, fisheries accounted for 44.5% of gross domestic product (Zeller and Reinert 2004), and its traditional pilot whale hunt provides approximately 30% of total meat consumed on the islands (Faroe Government 2004). Although the whale hunts are important in terms of cultural identity and food security, there is also concern that the contaminant burden in whales could be detrimental to human health.

In the 1990s, it was found that children who were exposed prenatally to elevated levels of methylmercury suffered cognitive impairment (Grandjean et al. 1992, 1997). Subsequent studies also provided evidence of attenuated postnatal growth due to the transfer of methylmercury from mother to child during breastfeeding. In response to these findings, pregnant Faeroese women were reported to have decreased the amount of whale meat and fish in their diet (Weihe et al. 2003). Methylmercury exposure levels were assessed for the general population and for pregnant women, and these exposure levels were compared with the tolerable weekly intake levels advised by both the World Health Organization (WHO) and the EPA. Also of concern is the impact climate change may have on the accumulation of methylmercury: Increased temperatures lead to increased methylation rates, making increased amounts of methylmercury available. Therefore, increasing exposure levels would be expected to be found in human populations relying on marine resources as part of their diet.

Using EwE, an ecosystem model was constructed for the Faeroe Islands EEZ, and the flow of methylmercury was described via the Ecotracer routine (Booth and Zeller 2005). The human exposure to methylmercury via consumption of cod and pilot whale meat

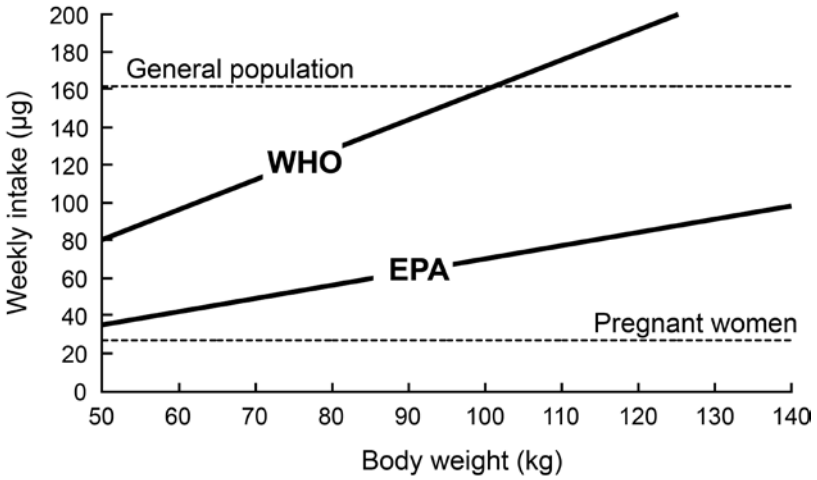

Figure 13.2. Weekly intake of methylmercury for the general population in the Faeroes and for pregnant women who lowered their intake of pilot whale and cod, the two marine species dominant in the traditional diet. People who weigh less than approximately 100 kg are above the WHO and EPA TWI limits, and pregnant women who lowered their weekly intake of pilot whale and cod are below the WHO and EPA TWI limits, irrespective of body weight. (Modified from Booth and Zeller 2005.)

was examined, the two main marine species providing most protein in the traditional diet. The environmental concentration was increased from 3.3 to 3.6 g/km^2 over 100 years to approximate the increase in the amount of methylmercury in the water column since the onset of the Industrial Revolution (Mason and Sheu 2002). The base inflow rate was considered to be only from atmospheric deposition and a value of 0.113 g/km^2/year was used (Downs et al. 1998). In the first hundred years of the simulation, biotic groups and the environment were allowed to equilibrate to "present" conditions so that the predicted concentrations from the model simulation fell within the range of reported values. To assess the impacts of changes in fishing mortality rates and the effects of increasing methylation rates as a result of climate change on the ecosystem, a second simulation was undertaken from the present to 100 years in the future. We investigated the results of ocean temperature changes of 0.4°C and 1.0°C per century, the range expected by the International Panel on Climate Change (IPCC 2001). Changes in fishing and whaling mortality rates of 20% were also simulated on all targeted species, and the combined effects of climate change and changes in mortality rates were also investigated.

Methylmercury exposure levels based on the consumption of 12 g of pilot whale meat per week and 72 g of cod per week for the general population (Vestergaard and Zachariassen 1987) were compared with the tolerable weekly intake (TWI) limits set by the WHO of 1.6 µg/kg body weight and to the more risk-averse EPA value of 0.7 µg/kg body weight.[2] Weekly intake levels were also assessed for pregnant women who lowered their consumption to 1.45 g of pilot whale meat per week and 40.2 g of cod per week (Weihe et al. 2005). Model results indicate that women who changed their diets are below the limits set by the WHO and the EPA under both climate change scenarios and under the scenarios of changing fishing mortality rates. However, currently and under all scenarios the general population is above the methylmercury exposure levels set by the EPA, but for the WHO limits, the results depend on a person's body weight. Currently, people who weigh less than 102 kg and consume the reported average amount of pilot whale and cod are above the WHO limit, and under both climate change scenarios more people would be above the limit (figure 13.2).

Changes in the fishing and whaling mortality rates affected the concentration of methylmercury in the species and functional groups. Decreasing mortality rates on tar-

geted species and functional groups led to an increase in biomass for the targeted species, but the prey items of these groups in the simulation showed a decrease in methylmercury concentrations. Decreasing the fishing and whaling mortality rates on targeted species, in the model simulation, leads to a decrease in the production/biomass (P/B) ratio, lowering the turnover rate of the population, and has the effect of extending longevity, allowing a longer time for accumulation to occur in the targeted species. However, simulating an increase in biomass for the targeted species also has the effect of decreasing the longevity of targeted species' prey items, thus lowering methylmercury concentrations in prey groups. Increasing mortality rates on targeted species had the opposite effect: lowered methylmercury concentrations in targeted species and groups, with consequential increases in concentrations of methylmercury in their prey items.

GLOBAL MODELS

Bioaccumulation of Dioxin

A global model involving spatial data was developed to describe the movement of dioxin up through the marine food web of the global oceans using the Ecospace and Ecotracer routines of the EwE modeling routine (Christensen and Booth 2006). It uses input data from a preliminary spatial dioxin ocean loading model as a result of atmospheric depositions (Zeller et al. 2006). Studies looking at the effects of dioxin in marine ecosystems are lacking, with most studies examining only concentrations in species of concern.

The underlying Ecopath model includes forty-two functional groups and is based on a modified model (Generic 37) developed for database-driven model construction distributed with the EwE software. The ecosystem is represented by a grid of 2° latitude × 2° longitude cells and extends from the equator to 70° latitude north and south. The oceans are divided into two depth zones (<200 m, >200 m), and most functional groups were assigned to both zones, except for small demersal fishes, reef fishes, seals, corals, and benthic plants, which were assigned to the shallower depth zone. Functional groups were assigned to all nineteen FAO statistical areas, and the groups were assigned primarily on estimates of primary production.

The modeling approach involved using predation, catches, and an assumed ecotrophic efficiency to estimate the biomass of each functional group. Default values for the Generic 37 model were maintained, but density levels were assigned for large sharks (0.1 t/km^2), jellyfish (0.1 t/km^2), seals and other pinnipeds (0.003 t/km^2), toothed whales (0.002 t/km^2), baleen whales (0.001 t/km^2), seabirds (0.001 t/km^2), macrobenthos and meiobenthos (1.5 and 2 t/km^2, respectively), corals (1 t/km^2), soft corals and sponges (2 t/km^2), and benthic plants (10 t/km^2). Catch data for each functional group were taken from the *Sea Around Us* and represent the catch taken in 2000. Spatially explicit data used in the Ecospace routine include primary production, biomass estimates for zooplankton, macrobenthos and meiobenthos, small and large mesopelagic fishes, and depth information for each half-degree spatial *Sea Around Us* cell.

Concentrations of dioxin in marine organisms were sourced mainly from the primary literature and represent reported values since 1990 in toxic equivalencies (TEQs). Seventeen congeners of dioxin have been reported as being toxic, and data reported as individual congeners were transformed into TEQs using the appropriate toxic equivalency factors (TEFs; Van den Berg et al. 1998). Concentrations in marine mammals were standardized to ng/kg lipid weight, and those for other organisms were standardized to ng/kg wet weight. Species with reported values were sorted into their respective functional groups and were placed within their representative region.

In the oceans, direct uptake rates of dioxin by primary producers and invertebrates are an important pathway for the transfer of pollutants up the food web. However, because of the lack of data on uptake rates, we assume that the dioxin is taken up only by phytoplankton once deposited to the ocean, and to prevent the

Table 13.2. Starting values used in the Ecotracer routine for the environment and biota.

Ecotracer inputs	Value
Initial concentration	0.1 t/km²
Base inflow rate	1.0 t/km²/year
Decay rate	1.0/year
Phytoplankton uptake rate	0.5 t dioxin/t in environment/t phytoplankton/year

accumulation of dioxin in the oceans, a decay rate was used for the environment (table 13.2). Thus, concentrations in the biota are a result of uptake of dioxin by phytoplankton and trophic transfer through the food web with no decay in biota. Under these initial conditions, the simulation was run for 22 years, and the results from the model were compared with the reported concentration values.

After the simulation was run, most groups reached equilibrium dioxin concentrations, excluding the whales (baleen and toothed), seals, and bird groups, which are long-lived (figure 13.3).

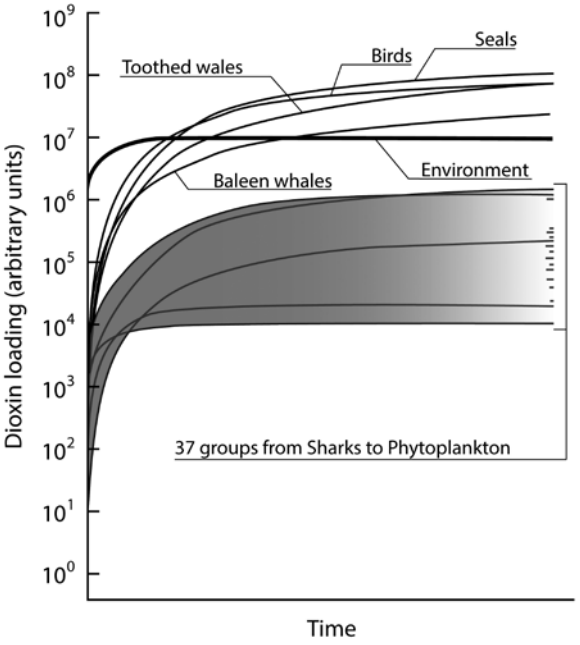

Figure 13.3. Predicted concentrations of dioxin in the global marine ecosystem model for each functional group, listed in order of highest to lowest values (top to bottom). At the end of the 22-year simulation, equilibrium had been reached in most functional groups, excluding whales (toothed and baleen), seals, and birds. (Adapted from Christensen and Booth 2006.)

Excluding four outliers, the regression between predicted and observed dioxin concentrations explains 25% of the variation in the sample values ($p << 0.001$; figure 13.4) with a slope value of 0.84. Of the four outliers, two were associated with the polar regions, and the other two were associated with coastal areas in Asia. Predicted values for polar regions may be affected by both the duration of the atmospheric model (one year) and nonconsideration of reemission of dioxin from land back to the atmosphere caused by the "grasshopper effect" (Wania and Mackay 1996). Values for the coastal regions in Asia may also be affected by the input from coastal runoff and riverine outflow. The grasshopper effect and nonatmospheric inputs are not included in the preliminary atmospheric transport and deposition model of dioxin (but they were considered in the deposition models further below).

An important outcome of using a global EwE model with the Ecospace routine is that Ecotracer can predict the observed values of dioxin, although only within two orders of magnitude. The predictive power could be improved by having larger sample sizes for underrepresented areas. Because most concentration values are reported from coastal areas in developed countries (figure 13.5), samples from depths greater than 200 m and from developing areas could lead to a better fit. Improved fits may also be achieved by improving the atmospheric transport and deposition model to include the grasshopper effect, coastal runoff, and riverine inputs of dioxin, and these effects were considered in the updated atmospheric model for dioxin (see below).

Global Deposition of Atmospherically Released Dioxin

As a follow-up to the modeling work reported above, a global model of dioxin was developed that includes production, atmospheric diffusion and dispersion, transport from land to coastal waters, and depositions to land and oceans (Booth et al. 2013). Its purpose was to highlight the deposition of dioxin in marine

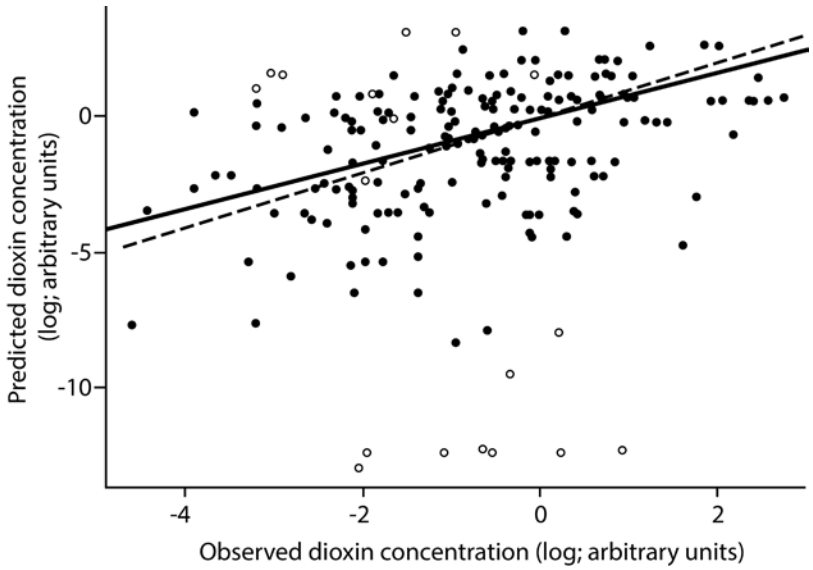

Figure 13.4. Predicted versus observed dioxin concentrations in various marine organisms (see text). The dashed line represents the case where the predicted values match the observed values, and the solid line is a fitted regression ($r^2 = 0.25$; $p < 1.7e^{-13}$). Open symbols are from 4 sample areas considered to be outliers and not included in the regression. (Adapted from Christensen and Booth 2006.)

areas including countries' EEZs and the high seas to improve models such as that presented previously on the bioaccumulation of dioxin in marine ecosystems. Dioxin concentrations measured in marine organisms result from the input of dioxin to the oceans, but dioxin is not measured in the water column, and thus organism concentrations and sediment concentrations have served as a proxy to indicate areas that are more affected by dioxin than others. Monitoring programs for dioxin concentrations in organisms are sparse, and developing countries lack the resources to properly monitor the impacts. Thus, this model, of which only an outline is presented here (but see Booth et al. 2013) identifies areas of potential concern, that is, where airborne dioxins are likely to be deposited.

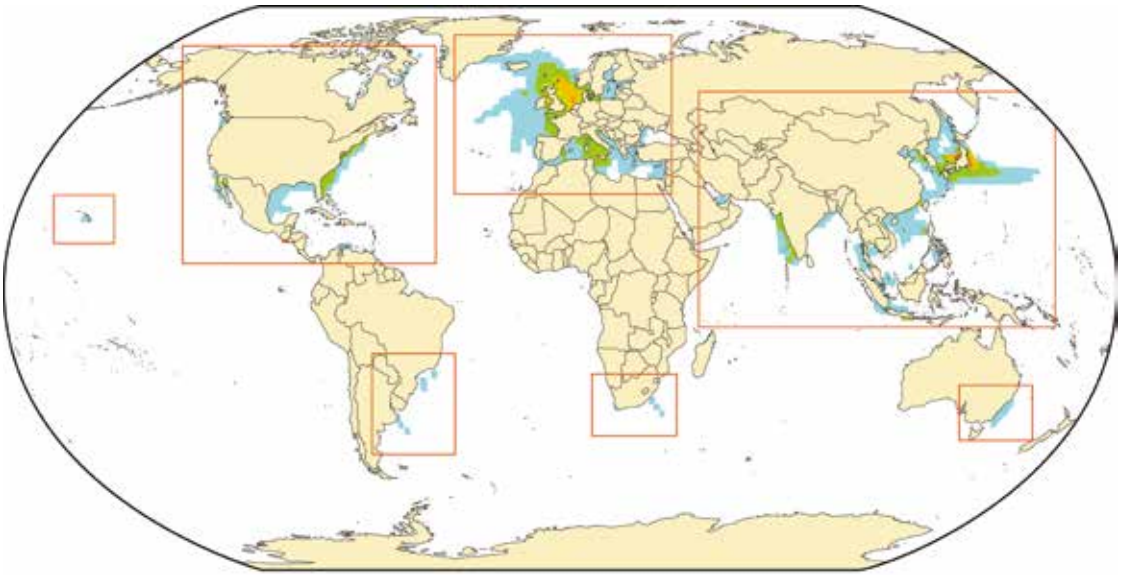

Figure 13.5. Predicted relative dioxin concentration in small pelagic fishes. Scale is from white to light blue to green, yellow, and orange. Note high concentrations in the waters around Asia, Europe, and North America, and lower concentrations in South America, Africa, and Australia. (Adapted from Christensen and Booth 2006.)

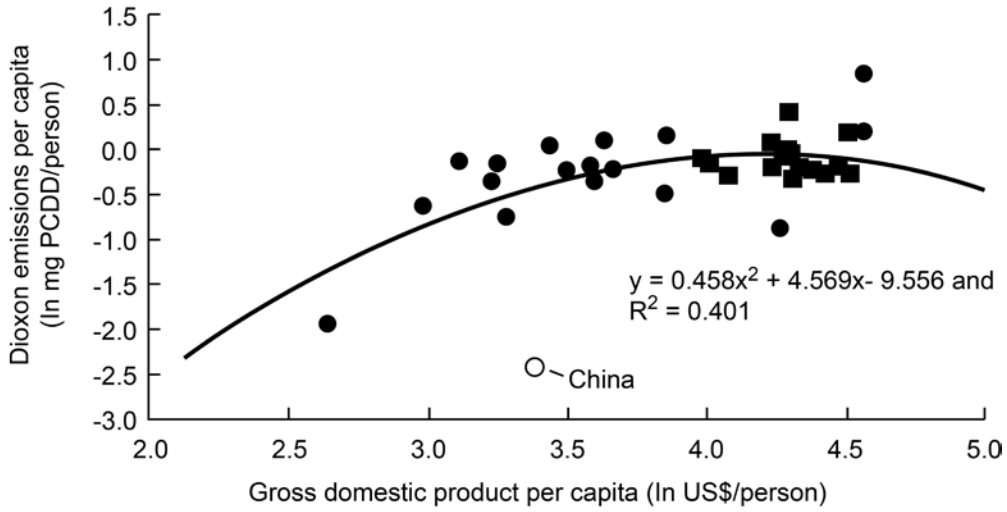

Figure 13.6. Environmental Kuznets curve used to estimate countries' per capita dioxin emissions. Original data used in Baker and Hites (2000) are shown in square symbols, new data are shown in circles, with China (open circle) omitted from analysis. (Adapted from Booth et al. 2013.)

A previous global mass balance of dioxin estimated global annual emissions of 13,100 kg ± 200 kg (Brzuzy and Hites 1996), which assumed that annual depositions to oceans contributed 5% to the global mass balance. In a preliminary run of our model we found that ocean depositions were approximately 38% and therefore increase global emissions to 17,226 kg. Mass balance studies have shown that depositions of dioxin are about ten times greater than reported emissions because of the formation of dioxin from pentachlorophenol, a common wood preservative, by photochemical transformation in the atmosphere (Baker and Hites 2000). Thus, each emission value was multiplied by 9.7 to account for this discrepancy, and the estimated annual emissions were considered to be released in weekly increments.

The production of dioxin for thirty-five countries was based on their reported inventories of annual atmospheric releases, with most of these countries having a single estimate between 1995 and 2002 (see Supplementary Online Material in Booth et al. 2013). The year 1998 was chosen as representative for the emission inventories, corresponding gross domestic product (GDP) data, and population data (see Chen 2004 for an example). Population data for each of the thirty-five countries were used to transform GDP and atmospheric releases of dioxin into per capita rates. The line of best fit through these points, representing an environmental Kuznets curve, was used to generate the atmospheric dioxin emissions for countries that have not completed a dioxin inventory (figure 13.6).

Within each country, we assigned dioxin emissions using spatial estimates of GDP. A global data set of spatialized estimates of GDP (Dilley et al. 2005) were mapped onto a global grid of half-degree cells, and dioxin emissions were then made directly proportional to the fraction that each land cell contributed to the country's total GDP per land area (i.e., GDP/km^2).

Dioxin dispersion in the atmosphere involved diffusion and the transport of dioxin with wind. Weekly releases of dioxin to the atmosphere were subjected to diffusion, using the diffusion constant for 2,3,7,8-TCDD dioxin of 4.86×10^{-6} m^2/s (Chiao et al. 1994), and to global wind patterns. Wind data consisted of global daily means of east–west and north–south wind components from the 40-year reanalysis dataset of the European Center for Medium-Range Weather Forecasts (2006). These data were further averaged over the 1991–2000 time period into weekly values.

The deposition of dioxin was simulated using the data in table 13.2 and the characteristic travel distance approach (CTD), which

describes the distance an airborne semivolatile organic pollutant travels before reaching 1/*e* (i.e., ~37%) of its initial value (Bennett et al. 1998). The temperature-dependent CTD, which accounts for the grasshopper effect, for 2,3,7,8-TCDD dioxin was used to estimate the amount of dioxin deposited from the atmosphere to land and water (Beyer et al. 2000). Because the distance traveled depends on temperature and wind speeds, we used the temperature-dependent CTD for 2,3,7,8-TCDD dioxin at 5°C, 15°C, and 25°C (Klasmeier et al. 2004) to derive a temperature-dependent CTD for temperatures greater than 0°C.

The CTD is described by wind speed and the effective decay rate,

$$CTD = \mu / k_{eff}, \qquad (13.1)$$

where μ is the wind speed (m/s) and k_{eff} (per second) is the effective decay rate. The effective decay rate accounts for the transfer of dioxin from air to land and water surfaces and to biological components (e.g., plants). Because each geographic information system (GIS) cell has the wind speed and temperature as an attribute, a temperature-dependent CTD is defined, and therefore we rearrange the equation to solve for the effective decay rate for each GIS cell,

$$k_{eff} = CTD / \mu . \qquad (13.2)$$

Water basin transport of dioxin from land to coastal marine areas was also simulated using water runoff amounts as the driver. Data kindly supplied by Dr. C. J. Vörösmarty of the Water Systems Analysis Group at the University of New Hampshire (www.wsag.unh.edu) describe a global total of 6,031 basins, with 5,865 basins identified as ultimately exiting to coastal marine waters and 166 identified as landlocked. To identify coastal cells that receive dioxin via water basin transport, salinity gradient plots were used to determine whether a basin's outflow created a freshwater plume in marine waters. For discharge areas that had plumes, dioxin was deposited into the cells that created the plume; for river discharge areas that did not have identifiable plumes, we specified a single central coastal cell to receive the dioxin. For regions between 0° and 65° latitude N or S, we used a salinity threshold of 30 psu to identify freshwater plumes, whereas for regions located above 65° latitude N or S, we used a salinity threshold of 25 psu because of the large inputs of freshwater that remain in surface waters in polar areas. Salinity data were taken from the World Ocean Atlas 2005 (Antonov et al. 2006).

Water runoff was shown to be the dominant pathway of dioxin transport in a Japanese watershed (Kanematsu et al. 2009), accounting for more than 98% of total dioxin transport. We used a proportionality constant of 0.0004/year, derived from two studies examining dioxin transport (Vasquez et al. 2004; Kanematsu et al. 2009), in combination with water runoff data for each water basin (Fekete et al. 2000) to transport dioxin from water basins to coastal marine cells.

We simulated the dispersion and deposition of airborne dioxin by a two-dimensional diffusion–advection differential equation:

$$\frac{\partial A}{\partial t} = \frac{\partial}{\partial x}\left(D\frac{\partial A}{\partial x}\right) + \frac{\partial}{\partial y}\left(D\frac{\partial A}{\partial y}\right) - \frac{\partial}{\partial x}(\mu * A) - \frac{\partial}{\partial x}(\nu * A) - \lambda * A, \qquad (13.3)$$

where *A* is the amount of dioxin in a grid cell, *D* is the diffusion coefficient (4.86×10^{-6} m²/s), μ and ν are the wind velocity components (in the N–S direction and E–W direction, respectively), and lambda (λ) is the decay rate (i.e., k_{eff}).

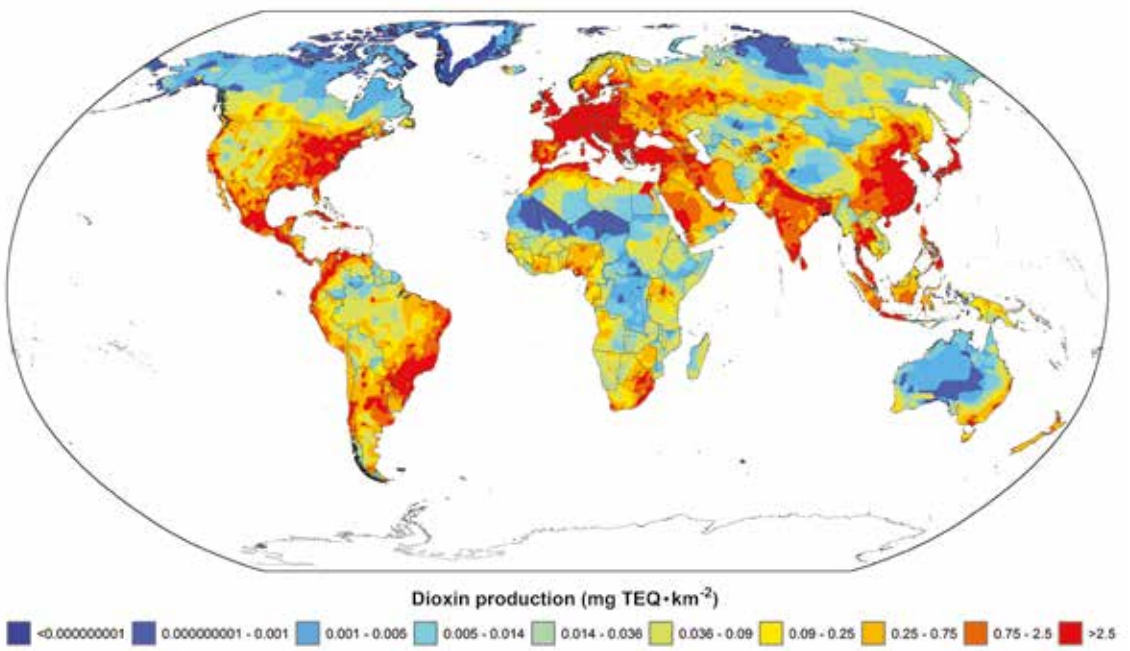

Figure 13.7. Global production of dioxin as toxic equivalents of 2,3,7,8-tetrachlorodibenzo-*p*-dioxin spatialized over the earth's surface, with emissions based on an environmental Kuznets curve. (Adapted from Booth et al. 2013.)

To numerically estimate the spatial and temporal amount of airborne dioxin above each cell, a finite difference technique using the alternating direction approach was used (Sibert and Fournier 1991). Briefly stated, the alternating direction approach requires that the amount of dioxin above each cell is determined by splitting each time step in half, determining the amount of dioxin at the end of the first half time step in a row-by-row fashion, and then determining the amount of dioxin at the end of each second half time step by column. Thus, we divided our 30-s time steps into two 15-s time steps and solved for the E–W and then the N–S movement. These two half time step processes were repeated for each time step in a week. To maintain mass balance, we redistributed any losses in the cumulative amount of dioxin in the system at the end of each time step, based on each cell's proportion of the overall total. The entire computation was repeated for each week of the year.

At the beginning of each week, each grid cell received its GDP-based share of global dioxin production, which was added to the amount that remained airborne at the end of the previous week. A circular boundary condition was also applied at all four edges of the global cell grid. In effect, this reconnected the cells in the rightmost column (i.e., 180°E longitude) to the cells of the same latitudes in the leftmost column (i.e., 180°W longitude). The application of the circular boundary condition also meant that the cells in the top row (i.e., 90°N latitude) were reconnected to those in the same row with a longitude difference of 180°. Similar reconnection of cells in the bottom row (i.e., 90°S latitude) also occurred.

For each cell, the amount of dioxin deposited to the earth's surface within each time step was determined as

$$\text{Dioxin deposited} = A * (1 - \exp[-(\omega/\text{CTD})(\text{ts})]), \quad (13.4)$$

where A is the amount of airborne dioxin above each cell, ω is the wind speed, CTD is the temperature-dependent characteristic travel distance, and ts is the time step (30 s).

The computer simulation of dioxin production suggested several areas of high local production of dioxin due to higher levels of

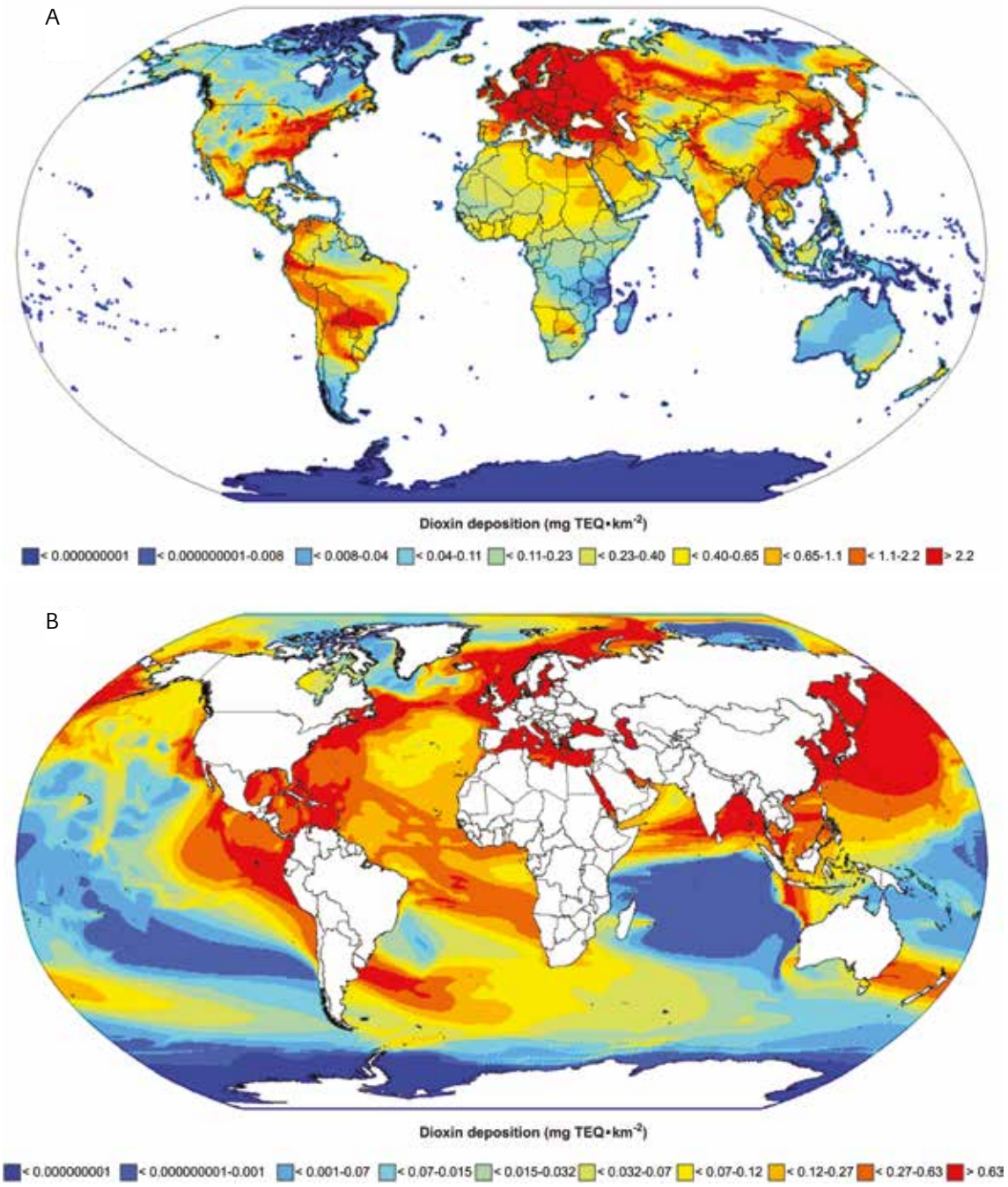

Figure 13.8. Deposits of dioxin to land (A) and to the world's oceans (B) presented as toxic equivalents of 2,3,7,8-tetrachlorodibenzo-*p*-dioxin after simulating 1 year of transport processes of global atmospheric emissions. (Modified from Booth et al. 2013.)

economic activity (figure 13.7). These were dominated by eastern North America, Europe, South Asia (particularly the Indian subcontinent), and East Asia (China, Japan, and South Korea). Countries belonging to the G20 account for more than 80% of the estimated annual emissions, with Japan, the United States, and China accounting for 30% of annual global emissions. However, it is smaller states such as Singapore and Malta that have the highest emissions per area.

After we ran the model to simulate 1 year's production, dispersion, deposition, and transport of dioxin, approximately 9 kg-TEQ (3%) of the annual dioxin production remained in the atmosphere. The model predicted that most of

the annual production of dioxin, 163 kg-TEQ (57%), was deposited to land areas, and ocean waters received approximately 115 kg-TEQ (40%). Large parts of North America, most of central, northern, and Eastern Europe, as well as much of the Indian subcontinent and East Asia have high terrestrial depositions of dioxins (figure 13.8A). Dioxin depositions to land range from 1×10^{-8} mg-TEQ/km^2 to 146 mg-TEQ/km^2, with the lower values in the Antarctic and the highest values found in Europe and South Korea.

The model also suggested that ocean areas near the source emission areas also received high dioxin loads. These include the northeast and northwest Atlantic, Caribbean, Mediterranean, northern Indian Ocean, and large parts of the northwestern Pacific and South China Seas (figure 13.8B). However, several areas of low concentration of dioxins were also identified, specifically parts of the west coast of South America and northern parts of the west coast of North America. Marine deposited dioxin ranged from 1×10^{-8} mg-TEQ/km^2 to 33.5 mg-TEQ/km^2 and were similar to terrestrial deposits in that lower values were associated with the Antarctic, but the highest values were found in waters off Japan and South Korea. High dioxin depositions were also found in the marine waters of countries around Baltic and Mediterranean Seas.

Dioxin deposited to the oceans results from the production of dioxin on land, and thus the oceans can act as a sink for dioxin. The high seas receive the largest amount of dioxin (~36 kg-TEQ) as modeled here, and once standardized by area, depositions to the high seas are approximately 0.16 mg-TEQ/km^2. The most affected countries when comparing the ratio of deposits to emissions were found in Africa and Asia. Of the top twenty affected countries, eleven are located in Africa and six in Asia. The eleven African countries' per capita GDPs average less than US$250/person/year, and the Asian countries average less than US$450/person/year.

This work provides the opportunity to examine the impacts of dioxin on marine ecosystems. Coastal shelves provide most of the fish destined for human consumption (Pauly et al. 2002), and some coastal ecosystems (e.g., eastern North America, China, and Europe) receive much larger dioxin loads than other marine areas (e.g., most of South America and Australia). Past research has shown that dioxin levels in fish oils derived from forage fish around Europe and eastern North America have higher concentrations than those sourced from Peru (FAO 2002; Hites et al. 2004). We would expect a similar relationship for all ecosystem components, with higher concentrations found in places that receive higher inputs of dioxin.

Our model suggests that the oceans are strongly affected by dioxin. Previously, it was assumed that the ocean received only about 5% of the global annual production of dioxin (Baker and Hites 2000). Using spatial and temporal distributions of dioxin emissions in a kinematic model, we have shown that the oceans receive approximately 40% of the annual deposits. Although much of this is confined to coastal areas, the impacts on the high seas are not negligible and have consequences for food security. One concern is that dioxin is more likely to partition to plastic particles that are eaten by marine plankton and fishes, an entry point for accumulation (Rios et al. 2010). Thus, human populations with high seafood consumption levels may be exposed to higher levels of dioxin than previously thought.

This model does not account for direct (i.e., nonatmospheric) releases of dioxin to land or water, and this contributes to the lack of mass balance between emissions and depositions for dioxin. However, using the Kuznets curve for dioxin emissions lowers the mass balance discrepancy factor from 12.5 to 9.7. Polar regions receive little dioxin over the model simulation time of 1 year, but these areas may be affected by the accumulation of this toxin over longer time periods. Simulations that were run for a longer duration would show higher levels of dioxin in polar regions as dioxin migrated poleward as a result of the grasshopper effect.

CONCLUSIONS

The concepts, approaches, and results presented in this chapter illustrate that marine pollution studies, which are often performed in isolation from other ecosystem studies, can profitably be conducted with modifications of standard tools used by marine and fisheries scientists (e.g., the EwE and EcoTroph approach and software briefly described in chapter 9). If this is done systematically, it may lead to studies of ecosystem functioning and on the impact of fisheries, also providing results on the effects of persistent organic and other pollutants on ecosystems, biodiversity, fisheries, and hence public health. Integrative studies of this kind, which, as illustrated here, can be performed on a global basis, would thus greatly contribute to providing policy-relevant results.

ACKNOWLEDGMENTS

This work was undertaken as part of the *Sea Around Us*, a research activity at the University of British Columbia initiated and funded by the Pew Charitable Trusts from 1999 to 2014 and currently funded mainly by the Paul G. Allen Family Foundation. We thank Douw Steyn, Xu Wei, and Jordan Dawe of the Department of Earth and Ocean Sciences at the University of British Columbia and Zoreida Alajado, Sherman Lai, and Joe Hui, formerly with the *Sea Around Us*, for their input and advice. We also thank Dr. Charles Vörösmarty of the Water Systems Analysis Group at the University of New Hampshire for global data on water basins.

REFERENCES

Aguilar, A., A. Borrell, and T. Pastor. 1999. Biological factors affecting variability of persistent pollutant levels in cetaceans. *Journal of Cetacean Research and Management* (Special Issue 1): 83–116.

Aguilar, A., A. Borrell, and P. J. H. Reijnders. 2002. Geographical and temporal variation in levels of organochlorine contaminants in marine mammals. *Marine Environmental Research* 53(5): 425–452.

AMAP. 1997. *Arctic pollution issues: a state of the Arctic environment report*. Arctic Monitoring and Assessment Programme (AMAAP), Oslo, Norway.

Antonov, J. I., R. A. Locarnini, T. P. Boyer, A. V. Mishonov, and H. E. Garcia. 2006. World ocean atlas 2005, volume 2: Salinity. Levitus, S. (ed). *NOAA Atlas NESDIS 62*, U.S. Government Printing Office, Washington, DC. Available at www.nodc.noaa.gov. Accessed December 2007.

Baker, J. I., and R. A. Hites. 2000. Is combustion the major source of polychlorinated dibenzo-*p*-dioxins and dibenzofurans to the environment? A mass balance investigation. *Environmental Science and Technology* 34: 2879–2886.

Becker, P. R. 2000. Concentration of chlorinated hydrocarbons and heavy metals in Alaska arctic marine mammals. *Marine Pollution Bulletin* 40(10): 819–829.

Bennett, D. H., T. E. McKone, M. Matthies, and W. E. Kastenberg. 1998. General formulation of characteristic travel distance for semivolatile organic chemicals in a multimedia environment. *Environmental Science and Technology* 32: 4023–4030.

Beyer, A., D. Mackay, M. Matthies, F. Wania, and E. Webster. 2000. Assessing long-range transport potential of persistent organic pollutants. *Environmental Science and Technology* 30: 1797–1804.

Booth, S., J. Hui, Z. Alojado, V. Lam, W. W. L. Cheung, D. Zeller, D. Steyn, and D. Pauly. 2013. Global deposition of airborne dioxin. *Marine Pollution Bulletin* 75(1–2): 182–186.

Booth, S., and D. Zeller. 2005. Mercury, food webs, and marine mammals: implications of diet and climate change for human health. *Environmental Health Perspectives* 113: 521–526.

Brzuzy, L. P., and R. A. Hites. 1996. Global mass balance for polychlorinated dibenzo-*p*-dioxins and dibenzofurans. *Environmental Science and Technology* 30(6): 1797–1804.

Bugoni, L., L. Krause, and M. V. Petry. 2001. Marine debris and human impacts on sea turtles in southern Brazil. *Marine Pollution Bulletin* 42(12): 1330–1334.

Carson, R. L. 1951. *The Sea Around Us*. Oxford University Press, Oxford, England.

Carson, R. L. 1962. *Silent Spring*. Houghton Mifflin Company, Boston.

Chen, C.-M. 2004. The emission inventory of PCDD/PCDF in Taiwan. *Chemosphere* 54: 1413–1420.

Chiao, F. F., R. C. Currie, and T. E. McKone. 1994. *Final draft report: intermediate transfer factors for contaminants found in hazardous waste sites: 2,3,7,8-tetrachlorodibenzo-*p*-dioxin (TCDD)*. Risk Science Program (RSP), Department of Environmental Toxicology, University of California, Davis, CA.

Christensen, V., and S. Booth. 2006. Ecosystem modeling of dioxin distribution patterns in the marine environment. Pp. 83–102 in J. Alder and D. Pauly (eds.), *On the multiple uses of forage fish: from ecosystems to markets*. Fisheries Centre Research Reports 14(3), University of British Columbia, Vancouver, Canada.

Christensen, V., and C. J. Walters. 2004. Ecopath with Ecosim: methods, capabilities and limitations. *Ecological Modelling* 172: 109–139.

Coombs, A. P. 2004. *Marine mammals and human health in the eastern Bering Sea: using an ecosystem-based food web model to track PCBs*. MSc thesis, University of British Columbia, Resource Management and Environmental Studies, Vancouver, Canada.

Dilley, M., R. S. Chen, U. Deichmann, A. L. Lerner-Lam, and M. Arnold. 2005. *Natural disaster hotspots: a global risk analysis*. CIESIN and World Bank (unpublished data), Washington, DC.

Downs, S. G., C. L. MacLeod, and J. N. Lester. 1998. Mercury in precipitation and its relation to bioaccumulation in fish: a literature review. *Water Air Soil Pollution* 108: 149–187.

European Centre for Medium-Range Weather Forecasts. 2006. ECMWF 40-year reanalysis dataset. Available at http://data.ecmwf.int/data/index.html. Accessed February 2010.

FAO 2002. *Use of fishmeal and fish oil in aquafeeds: further thoughts on the fishmeal trap*, by M. B. New and U. N. Wijkström. FAO Fisheries Circular No. 975, Rome.

Faroe Government. 2004. *Whales and whaling in the Faroe Islands*. Available at: www.whaling.fo/index.htm (accessed June 2004).

Fekete, B., C. J. Vörösmarty, and W. Grabs. 2000. *Global, composite runoff fields based on observed river discharge and simulated water balances*. Available at www.grdc.sr.unh.edu. Accessed December 2007.

Grandjean, P., P. Weihe, P. J. Jørgensen, T. Clarkson, E. Cenichiari, and T. Viderø. 1992. Impact of maternal seafood diet on fetal exposure to mercury, selenium, and lead. *Archives of Environmental Health* 47(3): 185–195.

Grandjean, P., P. Weihe, R. F. White, F. Debes, S. Araki, K. Yokoyams, K. Murta, N. Sørensen, R. Dahl, and P. J. Jørgensen. 1997. Cognitive deficit in 7-year-old children with pre-natal exposure to methylmercury. *Neurotoxicology and Teratology* 19(6): 417–428.

Hites, R. A., J. A. Foran, D. O. Carpenter, M. C. Hamilton, B. A. Knuth, and S. J. Schwager. 2004. Global assessment of organic contaminants in farmed salmon. *Science* 303: 226–229.

IARC. 1997. *Polychlorinated dibenzo-p-dioxins and polychlorinated dibenzofurans: summary of data reported and evaluation*. International Agency for Research on Cancer (IARC) Monographs on the Evaluation of Carcinogenic Risks to Humans 69: 33.

IPCC. 2001. *Climate Change 2001: the scientific basis*. International Panel on Climate Change (IPCC), Cambridge University Press, Cambridge, UK. Available at www.grida.no/climate/ipcc_tar/wg1/htm. Accessed June 2004.

Iwata, H., S. Tanabe, N. Sakai, and R. Tatsukawa. 1993. Distribution of persistent organochlorines in the oceanic air and surface seawater and the role of ocean on their global transport and fate. *Environmental Science & Technology* 27(6): 1080–1098.

Iwata, H., S. Tanabe, M. Aramoto, N. Sakai, and R. Tatsukawa. 1994. Persistent organochlorine residues in sediments from the Chukchi Sea, Bering Sea and Gulf of Alaska. *Marine Pollution Bulletin* 28(12): 746–753.

Kanematsu, M., Y. Shimizu, K. Sato, S. Kim, T. Suzuki, B. Park, R. Saino, and M. Nakamura. 2009. Origins and transport of aquatic dioxins in the Japanese watershed: soil contamination, land use, and soil runoff events. *Environmental Science and Technology* 43: 4260–4266.

Kannan, K., A. L. Blankenship, P. D. Jones, and J. P. Giesy. 2000. Toxicity reference values for the toxic effects of polychlorinated biphenyls to aquatic mammals. *Human and Ecological Risk Assessment* 6(1): 181–201.

Kawano, M., S. Matsushita, T. Inoue, H. Tanaka, and R. Tatsukawa. 1986. Biological accumulation of chlordane compounds in marine organisms from the northern North Pacific and Bering Sea. *Marine Pollution Bulletin* 17(11): 512–516.

Klasmeier, J., A. Beyer, and M. Matthies. 2004. Screening for cold condensation potential of organic chemicals. *Organohalogen Compounds* 66: 2406–2411.

Livingston, P. A., and L. L. Low. 1998. *Bering Sea ecosystem research: planning, coordination, and communication*. Quarterly Report, Feature Article for Alaska Fisheries Science Center, National Marine Fisheries Service.

Loughlin, T. R., and A. E. York. 2000. An accounting of the sources of Steller sea lion, *Eumetopias jubatus*, mortality. *Marine Fisheries Review* 62(4): 40–45.

Mantua, N. J., S. J. Hare, Y. Zhang, J. M. Wallace, and R. C. Francis. 1997. A Pacific interdecadal climate oscillation with impacts on salmon production. *Bulletin of American Meteorological Society* 78: 1069–1079.

Mason, R. P., and G.-R. Sheu. 2002. Role of the ocean in the global mercury cycle. *Global Biogeochemical Cycles* 16(4): 40.1–40.14.

Moore, C. J. 2008. Synthetic polymers in the marine environment: a rapidly increasing, long-term threat. *Environmental Research* 108(2): 131–139.

NRC. 1996. *The Bering Sea Ecosystem*. National Academy Press, Washington, DC.

Parker, W., and D. Dasher. 1999. Pathways, sources and distribution of contaminants in the Arctic and Alaska. Pp. 5–48 in M. J. Bradley (ed.), *Alaska Pollution Issues*. Alaska Native Epidemiology Center, Anchorage, AK.

Pauly, D., V. Christensen, S. Guénette, T. J. Pitcher, U. R. Sumaila, C. J. Walters, R. Watson, and D. Zeller. 2002. Towards sustainability in world fisheries. *Nature* 418: 689–695.

Pauly, D., V. Christensen, and C. Walters. 2000. Ecopath, Ecosim, and Ecospace as tools for evaluating ecosystem impact of fisheries. *ICES Journal of Marine Science* 57: 697–706.

Rios, L. M., P. R. Jones, C. Moore, and U. V. Narayan. 2010. Quantitation of persistent organic pollutants adsorbed on plastic debris from the North Pacific gyre's "eastern garbage patch." *Journal of Environmental Monitoring* 12: 2189–2312.

Sibert, J. R., and D. A. Fournier. 1991. Evaluation of advection–diffusion equations for estimation of movement patterns from tag recapture data. Pp. 108–121 in R. S. Shomura, J. Majkowski, and S. Langi (eds.), *Interactions of Pacific tuna fisheries*. Proceedings of the first FAO expert consultation on interactions of Pacific tuna fisheries. FAO Fisheries Technical Paper No. 36, Volume 1, FAO, Rome.

Simmonds, M. P., K. Haraguchi, T. Endo, F. Cipriano, S. R. Palumbi, and G. M. Troisi. 2002. Human health significance of organochlorine and mercury contaminants in Japanese whale meat. *Journal of Toxicology and Environmental Health, Part A* 65(17): 1211–1235.

Tanabe, S. 2002. Contamination and toxic effects of persistent endocrine disrupters in marine mammals and birds. *Marine Pollution Bulletin* 45(1–12): 69–77.

Trites, A. W., P. A. Livingston, S. Mackinson, M. C. Vasconcellos, A. M. Springer, and D. Pauly. 1999. *Ecosystem change and the decline of marine mammals in the eastern Bering Sea: testing the ecosystem shift and commercial whaling hypotheses*. Fisheries Centre Research Reports 7(1), University of British Columbia, Vancouver, Canada.

Tysban, A. V. 1999. The BERPAC project: development and overview of ecological investigations in the Bering and Chukchi Seas. Pp. 713–731 in T. R. Loughlin and K. Ohtani (eds.), *Dynamics of the Bering Sea*. University of Alaska Sea Grant, Fairbanks, AK.

Valoppi, L., M. Petreas, R. Donohoe, L. Sullivan, and C. Callahan. 1998. *Use of PCV congener and homologue analysis in ecological risk assessments*. Biological Technical Advisory Group, U.S. Environmental Protection Agency, San Francisco, CA.

Van den Berg, M., L. Birnbaum, A. T. C. Bosveld, B. Brunström, P. Cook, M. Feeley, J. P. Giesy, A. Hanberg, R. Hasegawa, S. W. Kennedy, T. Kubiak, J. C. Larsen, F. X. R. van Leeuwen, A. K. D. Liem, C. Nolt, R. E. Peterson, L. Poellinger, S. Safe, D. Schrenk, D. Tillitt, M. Tysklind, M. Younes, F. Waern, and T. Zacharweski. 1998. Toxic equivalency factors (TEFs) for PCBs, PCDDs, PCDFs for humans and wildlife. *Environmental Health Perspectives* 106(12): 775–792.

Vasquez, A. P., J. L. Regens, and J. T. Gunter. 2004. Environmental persistence of 2,3,7,8-tetrachlorodibenzo-*p*-dioxin in soil around Hardstand 7 at Egline Air Force Base, Florida. *Journal of Soils and Sediments* 4(3): 151–156.

Vestergaard, T., and P. Zachariassen. 1987. Fødslukanning 1981–82. *Frødskaparrit* 33: 5–18.

Wania, F., and Mackay, D. 1996. Tracking the distribution of persistent organic pollutants. *Environmental Science and Technology* 30(9): 390A–396A.

Weihe, P., P. Grandjean, and P. J. Jørgensen. 2005. Application of hair-mercury analysis to determine the impact of a seafood advisory. *Environmental Research* 97: 201–208.

Weihe, P., U. Steurwald, S. Taheri, O. Faero, A. S. Veyhe, and D. Nicolajsen. 2003. The human health program in the Faroe Islands: 1985–2001. Pp. 194–198 in B. Deutch and J. C. Hansen (eds.), *AMAP Greenland and the Faroe Islands 1997–2001*. Arctic Monitoring and Assessment Programme, Oslo, Norway.

Zeller, D., S. Booth, V. Lam, C. Close, and D. Pauly. 2006. Global dispersion of dioxin: a spatial dynamic model with emphasis on ocean deposition. Pp. 67–82 in J. Alder and D. Pauly (eds.), *On the multiple uses of forage fish: from ecosystems to markets*. Fisheries Centre Research Reports 14(3), University of British Columbia, Vancouver, Canada.

Zeller, D., and J. Reinert. 2004. Modelling spatial closures and fishing effort restrictions in the Faroe Islands marine ecosystem. *Ecological Modelling* 172: 403–420.

NOTES

1. Cite as Booth, S., W. W. L. Cheung, A. P. Coombs-Wallace, V. W. Y. Lam, D. Zeller, V. Christensen, and D. Pauly. 2016. Pollutants in the seas around us. Pp. 152–170 in D. Pauly and D. Zeller (eds.), *Global Atlas of Marine Fisheries: A Critical Appraisal of Catches and Ecosystem Impacts*. Island Press, Washington, DC.
2. The U.S. EPA reference dose is 0.1 µg/kg body weight/day.